

RANDOMIZED STRONG RECURSIVE SKELETONIZATION: SIMULTANEOUS COMPRESSION AND  
FACTORIZATION OF  $\mathcal{H}$ -MATRICES IN THE BLACK-BOX SETTING

Anna Yesypenko and Per-Gunnar Martinsson  
The University of Texas at Austin

**Abstract:** The hierarchical matrix ( $\mathcal{H}^2$ -matrix) formalism provides a way to reinterpret the Fast Multipole Method and related fast summation schemes in linear algebraic terms. The idea is to tessellate a matrix into blocks in such a way that each block is either small or of numerically low rank; this enables the storage of the matrix and the application of it to a vector in linear or close to linear complexity. A key motivation for the reformulation is to extend the range of dense matrices that can be represented. Additionally,  $\mathcal{H}^2$ -matrices in principle also extend the range of operations that can be executed to include matrix inversion and factorization. While such algorithms can be highly efficient for certain specialized formats (such as HBS/HSS matrices based on “weak admissibility”), inversion algorithms for general  $\mathcal{H}^2$ -matrices tend to be based on nested recursions and recompressions, making them challenging to implement efficiently. An exception is the *strong recursive skeletonization (SRS)* algorithm by Minden, Ho, Damle, and Ying, which involves a simpler algorithmic flow. However, SRS greatly increases the number of blocks of the matrix that need to be stored explicitly, leading to high memory requirements. This manuscript presents the *randomized strong recursive skeletonization (RSRS)* algorithm, which is a reformulation of SRS that incorporates the randomized SVD (RSVD) to simultaneously compress and factorize an  $\mathcal{H}^2$ -matrix. RSRS is a “black box” algorithm that interacts with the matrix to be compressed only via its action on vectors; this extends the range of the SRS algorithm (which relied on the “proxy source” compression technique) to include dense matrices that arise in sparse direct solvers. Moreover, RSRS leads to dramatically simpler data structures, faster execution time, and easier parallelization. RSRS is particularly effective when applied to geometries that have lower dimensionality than the ambient space (as when discretizing a boundary integral equation on a surface in  $\mathbb{R}^3$ ), as it enables off-diagonal blocks to be compressed using their actual numerical ranks, rather than the rank imputed by a proxy surface.

1. INTRODUCTION

Dense matrices that arise in mathematical physics often have internal structure that makes it possible to solve problems involving elliptic operators in linear or close to linear time. Early techniques such as the Fast Multipole Method exploited mathematical properties of the kernel function directly to enable the fast application of dense matrices to vectors. The  $\mathcal{H}^2$ -matrix methodology followed, and reinterpreted the FMM in linear algebraic terms, where a matrix is tessellated into blocks in such a way that each block is either small or of numerically low rank. This reinterpretation opened the door to linear complexity algorithms for a wider range of algebraic operations, including the matrix-matrix multiplication, and the construction of invertible factorizations.

The manuscript describes the algorithm *Randomized Strong Recursive Skeletonization (RSRS)* for simultaneously compressing and inverting an  $\mathcal{H}^2$ -matrix, given a means of applying the matrix and its adjoint to vectors. The precise problem formulation is this: Suppose that  $\mathbf{A}$  is an  $\mathcal{H}^2$ -matrix, and that you are given a fast method for applying  $\mathbf{A}$  and its adjoint  $\mathbf{A}^*$  to vectors. We then seek to build two “test-matrices”  $\mathbf{\Omega}$  and  $\mathbf{\Psi}$  with the property that the  $\mathcal{H}^2$  representation of  $\mathbf{A}^{-1}$  can be constructed from the set  $\{\mathbf{Y}, \mathbf{Z}, \mathbf{\Omega}, \mathbf{\Psi}\}$ , where

$$\mathbf{Y} = \mathbf{A}\mathbf{\Omega} \quad \text{and} \quad \mathbf{Z} = \mathbf{A}^*\mathbf{\Psi}.$$

RSRS is immediately applicable in a range of important environments. First, it can be used to derive a rank-structured representation of any integral operator for which a fast matrix-vector multiplication algorithm, such as the Fast Multipole Method [8, 9], is available. In this context,

RSRS will directly output an invertible factorization of the integral operator. Second, it can greatly simplify algebraic operations involving products of rank-structured or sparse matrices. As an illustration, the Dirichlet-to-Neumann (DtN) operator for a bounded domain can often be constructed using boundary integral equation techniques, with the overall action of the DtN operator calculated by applying an iterative solver combined with a post-processing step. RSRS would let us directly build and factorize the DtN operator. Relatedly, the perhaps key application of rank-structured matrix algebra is the acceleration of sparse direct solvers, as the dense matrices that arise during LU factorization are often rank structured [30, 16, 1, 18]. In the course of such a solver, a typical operation would be to form a Schur complement such as  $\mathbf{S} = \mathbf{B}(I, J)\mathbf{B}(J, J)^{-1}\mathbf{B}(J, I)$ , where  $I$  and  $J$  are two index sets. If  $\mathbf{B}(J, J)$  is an  $\mathcal{H}^2$ -matrix, then  $\mathbf{B}(J, J)^{-1}$  can easily be applied to vectors via an LU factorization. If, additionally,  $\mathbf{B}(I, J)$  and  $\mathbf{B}(J, I)$  are either sparse or rank structured, then  $\mathbf{S}$  can easily be applied to a vector. RSRS in this environment allows us to directly compute a factorization of  $\mathbf{S}$ , which is precisely what is needed in order to move the overall LU factorization forwards.

The fact that RSRS simultaneously compresses and inverts the matrix is a key feature of the algorithm. Previous work on black-box randomized algorithms for compressing rank structured matrices [22, 15, 13, 17] has approached the tasks of compression and inversion as two separate computational stages, with one executed before the other. This approach is very natural for rank structured formats based on “weak admissibility” (where all off-diagonal blocks of the matrix are treated as low rank) since in this case simple and exact inversion algorithms are available [4, 7, 29]. In the “strong admissibility” case (where only interactions between well separated parts of the computational domain are compressed), LU factorization or inversion are much more challenging tasks that require repeated recompression of off-diagonal blocks as the algorithm proceeds [2, 3, 25, 28]. This complication has greatly limited the appeal of direct solvers based on rank structured matrices for problems involving fully three dimension geometries where strong admissibility is essential.

In terms of prior work, RSRS draws on the randomized SVD (RSVD) for low rank approximation of matrices [10, 14, 20], and on earlier methods that apply the RSVD to the problem of reconstructing rank structured matrices from matrix-vector products [13, 15, 17, 22]. It in particular draws on ideas from the recent dissertation of James Levitt [12, 13]. Finally, it draws heavily from the prior work on strong recursive skeletonization, including the original work [25], and the more recent [27].

The manuscript is structured as follows: Section 2 surveys the key ideas underlying the RSVD and how they can be applied to simultaneously compress all the off-diagonal blocks of a rank structured matrix. Section 2 also introduces the core idea that is the main contribution of the present work. Section 3 introduces the interpolatory decomposition and shows how it can be used to solve simple linear systems involving rank deficiencies in their coefficient matrices. Section 4 introduces our interpretation of the Strong Recursive Skeletonization (SRS) algorithm. Section 5 describes Randomized Strong Recursive Skeletonization in full, and discusses refinements to the basic scheme. Section 6 presents numerical experiments that demonstrate how RSRS performs in terms of speed, memory requirements, and precision.

## 2. RANDOMIZED COMPRESSION AND FACTORIZATION OF RANK STRUCTURED MATRICES

In this section, we highlight the key methodological contributions of the manuscript for a simple model problem. For points  $\{\mathbf{x}_j\}_{j=1}^N$  shown in Figure 1, consider the  $N \times N$  matrix  $\mathbf{A}$  with entries

$$(1) \quad \mathbf{A}(i, j) = k(\mathbf{x}_i, \mathbf{x}_j)$$

given by a kernel function  $k$ , for instance  $k(\mathbf{x}, \mathbf{y}) = \log|\mathbf{x} - \mathbf{y}|$ . The singularity at  $x = y$  can be handled with an appropriate quadrature rule. The matrix (1) and its adjoint can be applied rapidly to vectors using the fast multipole method. The objective is to recover an *approximate*

representation of  $\mathbf{A}^{-1}$  using random sketches

$$(2) \quad \mathbf{Y} = \mathbf{A} \mathbf{\Omega}, \quad \mathbf{Z} = \mathbf{A}^* \mathbf{\Psi}, \quad \mathbf{\Omega}, \mathbf{\Psi} \sim \mathcal{N}(\mathbf{0}, \mathbf{I})$$

$\begin{matrix} N \times p & N \times N & N \times p \\ N \times p & N \times N & N \times p \end{matrix}$

using Gaussian test matrices  $\mathbf{\Omega}, \mathbf{\Psi}$ . We will discuss the needed number of samples later, but for now, consider that  $p \ll N$ . The material in Section 2.1 follows [10, 21, 26], while the techniques in Sections 2.2 and 2.3 are based on ideas in [12, 13].

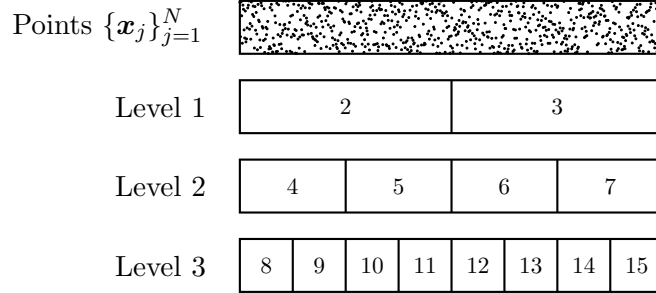


FIGURE 1. The hierarchical tessellation of boxes for a quasi one dimensional model problem. Boxes on the same level which share an edge or corner are called *neighbors*. Two boxes which are not neighbors are called *well-separated*. A box  $b$  has a *far-field* consisting of all boxes which are well-separated from  $b$ . As an example, box 9 has neighbors  $\{8,9,10\}$  and far-field  $\{11, \dots, 15\}$ .

The methodology uses that  $\mathbf{A}$  has certain rank deficiencies to recover a sparse factorization of  $\mathbf{A}^{-1}$  efficiently. Consider the tessellation of points into boxes 8,  $\dots$ , 15 on Level 3 of Figure 1, where each box has  $m := N/8$  points. The matrix  $\mathbf{A}$  has the following property for interactions between far-field blocks

$$(3) \quad \mathbf{A}_{i,j} \approx \mathbf{Q}_i \tilde{\mathbf{A}}_{ij} \mathbf{U}_j^*$$

$\begin{matrix} m \times m & m \times k & k \times k & k \times m \end{matrix}$

where index set  $I_i$  and  $I_j$  correspond to the indices of points of well-separated colleague boxes  $i$  and  $j$ , respectively. The low rank property of far-field interactions in (3) is depicted in Figure 2a. The blocks corresponding to interactions between near neighbors are stored densely.

In the next sections, we discuss methods for recovering the bases  $\mathbf{Q}_i$  and  $\mathbf{U}_j$ , which we call *block nullification*, in the black-box setting of (2). We also discuss techniques for recovering block-sparse interactions (e.g. interactions between near neighbors), which we call *block extraction*. First, to provide context, we review standard methods for recovering globally low-rank factors from matrix-vector products.

**2.1. Review of randomized sketching for a low rank matrix.** Suppose we would like to compute a low-rank approximation to the matrix  $\mathbf{A} \in \mathbb{R}^{m \times n}$  where the rank  $k$  is approximate and known apriori. Randomized low rank compression provides a powerful set of techniques for accomplishing this task via the action of  $\mathbf{A}$  and its adjoint on a small number of vectors.

A low rank approximation to  $\mathbf{A}$  can be computed in two stages. First, we would like to compute  $\mathbf{Q} \in \mathbb{R}^{m \times k}$  with orthonormal columns for which  $\mathbf{A} \approx \mathbf{Q} \mathbf{Q}^* \mathbf{A}$ . Once  $\mathbf{Q}$  is known, then we can form the matrix  $\mathbf{B} = \mathbf{A}^* \mathbf{Q}$  and the low-rank factorization of  $\mathbf{A}$  takes the form

$$(4) \quad \mathbf{A} = \mathbf{Q} \mathbf{B}$$

$\begin{matrix} m \times n & m \times k & k \times n \end{matrix}$

To find an approximate basis for the range of  $\mathbf{A}$  (e.g. find  $\mathbf{Q}$  such that  $\mathbf{A} \approx \mathbf{Q} \mathbf{Q}^* \mathbf{A}$ ), we generate a randomized sketch of  $\mathbf{A}$

$$(5) \quad \mathbf{Y} = \mathbf{A} \mathbf{\Omega}, \quad \mathbf{\Omega} \sim \mathcal{N}(\mathbf{0}, \mathbf{I}),$$

$\begin{matrix} m \times (k+l) & m \times n & n \times (k+l) \end{matrix}$

where  $l$  is a small oversampling parameter (e.g.  $l = 5$ ). The sketch  $\mathbf{Y}$  approximately spans the column space of  $\mathbf{A}$ , and desired orthonormal basis  $\mathbf{Q}$  can be computed by running a procedure to orthonormalize  $\mathbf{Y}$

$$(6) \quad \underset{m \times (k+l)}{\mathbf{Q}} = \text{orth}(\mathbf{Y}), \quad \text{where } \mathbf{Y} = \mathbf{Q}\mathbf{R}$$

When the rank  $k$  is not known a priori, there are adaptive algorithms available which build a low rank representation of  $\mathbf{A}$  from successive sketches. Randomized sketching methods can be used to construct a wide range of decompositions, including the interpolative decomposition which we introduce in Section 3.2. These algorithms are especially useful in the black-box setting of (2) because the matrix  $\mathbf{A}$  is only accessed through its action on vectors. In the next section, we discuss a modification of randomized low rank matrices which can be used to recover the orthogonal bases for the row and column blocks of (3).

**2.2. Block Nullification.** In the black-box setting of (2), we would like to recover the bases  $\mathbf{Q}_i, \mathbf{U}_i \in \mathbb{R}^{m \times k}$  for all blocks  $i = 8, \dots, 15$  as defined in (3). Consider that we do this using some modification of randomized sketching methods. Let the test and sketch matrices be tessellated according to the tree decomposition in Figure 1 on Level 3, so that

$$(7) \quad \mathbf{Y} = \begin{pmatrix} \mathbf{Y}_8 \\ \mathbf{Y}_9 \\ \vdots \\ \mathbf{Y}_{15} \end{pmatrix}, \quad \mathbf{\Omega} = \begin{pmatrix} \mathbf{\Omega}_8 \\ \mathbf{\Omega}_9 \\ \vdots \\ \mathbf{\Omega}_{15} \end{pmatrix}, \quad \mathbf{Y}_i \in \mathbb{R}^{m \times p}, \quad \mathbf{\Omega}_i \in \mathbb{R}^{m \times p}$$

and similar tessellations for  $\mathbf{Z}, \mathbf{\Psi}$ .

The structure of  $\mathbf{A}$  has dense interactions between near neighbor blocks, c.f. Figure 2a, which complicate the use of randomized sketching techniques. Ideally, the structure of the test matrices  $\mathbf{\Omega}$  would correspond to the sparsity pattern of the low rank blocks that we need to sample. Consider a ‘structured’ test matrix  $\mathbf{\Omega}' \in \mathbb{R}^{N \times k}$  for sampling the far-field of block  $i = 9$ , where  $\mathbf{\Omega}'_8, \mathbf{\Omega}'_9, \mathbf{\Omega}'_{10} = \mathbf{0}$  and the other blocks are Gaussian random matrices. Then sketching to produce  $\mathbf{Y}' = \mathbf{A}\mathbf{\Omega}'$ , extracting the  $I_9$  block, and post-processing would yield a basis for  $\mathbf{Q}_9$ :

$$(8) \quad \underset{m \times k}{\mathbf{U}_9} = \text{orth}(\underset{m \times k}{\mathbf{Y}'_9}), \quad \text{where } \underset{N \times k}{\mathbf{Y}'} = \underset{N \times N}{\mathbf{A}} \underset{N \times k}{\mathbf{\Omega}'}$$

To recover the basis for  $i = 12$ , another structured test matrix  $\mathbf{\Omega}'' \in \mathbb{R}^{N \times k}$  can be designed with zero blocks  $\mathbf{\Omega}''_{11}, \mathbf{\Omega}''_{12}, \mathbf{\Omega}''_{13} = \mathbf{0}$  and procedure in (8) can be repeated for the sketch  $\mathbf{Y}'' = \mathbf{A}\mathbf{\Omega}''$ . Using these structured test matrices, tailored for sampling the far field of every box, would require  $\frac{k}{m}N$  total samples and  $k^2N$  post-processing cost.

Block nullification accomplishes the same aim with much fewer samples and slightly increased post-processing costs. Let us again consider sampling the far-field of box  $i = 9$ , and consider that we construct a matrix  $\mathbf{N}'$  from the fully dense test matrix  $\mathbf{\Omega}$  defined in (7)

$$(9) \quad \underset{p \times (p-3m)}{\mathbf{N}'} = \text{null} \begin{pmatrix} \mathbf{\Omega}_8 \\ \mathbf{\Omega}_9 \\ \mathbf{\Omega}_{10} \end{pmatrix}$$

where the operation `null` gives an orthogonal basis for the nullspace of matrix. Suppose that  $p = (3m + k)$ , then  $\mathbf{N}'$  is  $k$ -dimensional with high probability. Multiplying  $\mathbf{N}'$  on the right of  $\mathbf{\Omega}$

gives

$$(10) \quad \begin{matrix} \mathbf{\Omega} & \mathbf{N}' \\ N \times p & p \times k \end{matrix} = \begin{pmatrix} \mathbf{\Omega}_8 & \mathbf{N}' \\ m \times p & p \times k \\ \mathbf{0} \\ \mathbf{0} \\ \mathbf{0} \\ \mathbf{\Omega}_{11} \mathbf{N}' \\ \vdots \\ \mathbf{\Omega}_{15} \mathbf{N}' \end{pmatrix} = \begin{pmatrix} \mathbf{\Omega}'_8 \\ m \times k \\ \mathbf{0} \\ \mathbf{0} \\ \mathbf{0} \\ \mathbf{\Omega}'_{11} \\ \vdots \\ \mathbf{\Omega}'_{15} \end{pmatrix} := \mathbf{\Omega}' \in \mathbb{R}^{N \times k},$$

where  $\mathbf{\Omega}'$  is the ‘structured’ Gaussian random matrix discussed earlier. The blocks  $\mathbf{\Omega}'_9, \mathbf{\Omega}'_{10}, \mathbf{\Omega}'_{11}$  are zero matrices by construction. Likewise, the structured random matrix  $\mathbf{\Omega}''$  for sampling the far field for  $i = 12$  can be constructed in a similar fashion.

$$(11) \quad \begin{matrix} \mathbf{\Omega} & \mathbf{N}'' \\ N \times p & p \times k \end{matrix} := \begin{matrix} \mathbf{\Omega}'' \\ N \times k \end{matrix}, \text{ where } \begin{matrix} \mathbf{N}'' \\ p \times (p-3m) \end{matrix} = \text{null} \begin{pmatrix} \mathbf{\Omega}_{11} \\ \mathbf{\Omega}_{12} \\ \mathbf{\Omega}_{13} \end{pmatrix}$$

To recover  $\mathbf{Q}_9$  as described in (8), we need the  $I_9$  block of the sketch  $\mathbf{Y}'$ , which we can construct by post-processing  $\mathbf{\Omega}$

$$(12) \quad \begin{matrix} \mathbf{Y}' \\ N \times k \end{matrix} = \begin{matrix} \mathbf{A} & \mathbf{\Omega}' \\ N \times N & N \times k \end{matrix} = \begin{matrix} \mathbf{A} \\ N \times N \end{matrix} \begin{pmatrix} \mathbf{\Omega} & \mathbf{N}' \\ N \times p & p \times k \end{pmatrix} = \begin{matrix} \mathbf{Y} & \mathbf{N}' \\ N \times p & p \times k \end{matrix}.$$

Note that because we only need the  $I_9$  block, the full sketch  $\mathbf{Y}'$  does not need to be formed explicitly. Instead,  $\mathbf{Y}'_9$  can be constructed as

$$(13) \quad \begin{matrix} \mathbf{Y}'_9 \\ m \times k \end{matrix} = \begin{matrix} \mathbf{Y}_9 & \mathbf{N}' \\ m \times p & p \times k \end{matrix}, \quad \text{then } \mathbf{Q}_9 = \text{orth}(\mathbf{Y}'_9).$$

Likewise, the basis  $\mathbf{Q}_{12}$  can be recovered by computing  $\mathbf{N}''$  as in (11) and orthonormalizing the sketch  $\mathbf{Y}''_{12} = \mathbf{Y}_{12} \mathbf{N}''$ . Block nullification allows us to recover all bases  $\mathbf{Q}_8, \dots, \mathbf{Q}_{15}$  using only  $p = (3m + k)$  samples of  $\mathbf{A}$  and  $\mathcal{O}((m^2 + m^2k)N)$  post-processing cost. The big-O notation hides constants related to the geometry which are discussed in a later section. The bases  $\mathbf{U}_8, \dots, \mathbf{U}_{15}$  can be recovered using a similar procedure for post-processing  $\mathbf{Z}$  and  $\mathbf{\Psi}$ .

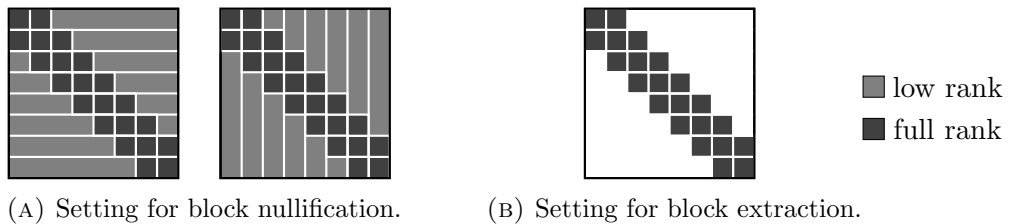


FIGURE 2. The figure depicts a rank-structured matrix  $\mathbf{A}$  in two settings. Figure 2a shows a dense matrix  $\mathbf{A}$  that uses low rank bases for each row and column block. Blocks which are well-separated, according to the geometry in Figure 1, are compressed using uniform bases, c.f. (3) for a formal definition. Figure 2b shows a special case of a rank-structured matrix, where the well-separated blocks have rank exactly 0.



**2.4. Factorizing  $\mathbf{A}$  using Randomized Sampling Techniques.** The objective of this work is to compute an invertible factorization of  $\mathbf{A}$ . The details of this machinery are discussed in subsequent sections. For now, assume the factorization takes the following form

$$(19) \quad \mathbf{A} = \mathbf{V}_8 \dots \mathbf{V}_{15} \tilde{\mathbf{A}} \mathbf{W}_{15} \dots \mathbf{W}_8,$$

where  $\tilde{\mathbf{A}}$  is block-diagonal. The matrices  $\mathbf{V}_i, \mathbf{W}_i$  for  $i = 8, \dots, 15$  diagonalize the row interactions and the column interactions of the block  $i$ . In the subsequent sections, we describe the operators  $\mathbf{V}_i$  and  $\mathbf{W}_i$ , but for this discussion, it is important to note that they are sparse and easy to invert.

Consider the following simpler decomposition of  $\mathbf{A}$ , which only includes the diagonalization operators for block  $i = 8$

$$(20) \quad \mathbf{A} = \mathbf{V}_8 \hat{\mathbf{A}} \mathbf{W}_8,$$

where  $\hat{\mathbf{A}}$  is defined in terms of the factorization of (19). In later sections, we will describe how  $\mathbf{V}_8$  and  $\mathbf{W}_8$  can be recovered using only a small number of random sketches (2) of the operator  $\mathbf{A}$  and its adjoint by post-processing  $\{\mathbf{Y}, \mathbf{\Omega}, \mathbf{Z}, \mathbf{\Psi}\}$ .

Suppose that  $\mathbf{V}_8$  and  $\mathbf{W}_8$  have been recovered and that we would like to use similar techniques to recover the operators  $\mathbf{V}_9$  and  $\mathbf{W}_9$ . Then, it would be natural to compute random sketches of  $\hat{\mathbf{A}}$

$$\hat{\mathbf{Y}} = \hat{\mathbf{A}} \hat{\mathbf{\Omega}}, \quad \hat{\mathbf{Z}} = \hat{\mathbf{A}}^* \hat{\mathbf{\Psi}}$$

and post-process  $\{\hat{\mathbf{Y}}, \hat{\mathbf{\Omega}}, \hat{\mathbf{Z}}, \hat{\mathbf{\Psi}}\}$ . A key observation of this manuscript, is that it is *not necessary to draw sketches* of  $\hat{\mathbf{A}}$  because the matrix can be written in terms of  $\mathbf{A}$  as

$$\hat{\mathbf{A}} = \mathbf{V}_8^{-1} \mathbf{A} \mathbf{W}_8^{-1}.$$

Instead, test and sketch matrices can be updated  $\{\mathbf{Y}, \mathbf{\Omega}, \mathbf{Z}, \mathbf{\Psi}\} \Rightarrow \{\hat{\mathbf{Y}}, \hat{\mathbf{\Omega}}, \hat{\mathbf{Z}}, \hat{\mathbf{\Psi}}\}$  using the following formulas

$$(21) \quad \begin{aligned} \hat{\mathbf{Y}} &= \mathbf{V}_8 \mathbf{Y}, & \hat{\mathbf{\Omega}} &= \mathbf{W}_8^{-1} \mathbf{\Omega} \\ \hat{\mathbf{Z}} &= \mathbf{W}_8^* \mathbf{Z}, & \hat{\mathbf{\Psi}} &= \mathbf{V}_8^{-*} \mathbf{\Psi} \end{aligned}$$

This observation allows us to sample the operator and its adjoint as in (2), then recover the factorization of  $\mathbf{A}$  by reusing the random sketches drawn initially.

### 3. THE INTERPOLATIVE DECOMPOSITION AND RECURSIVE SKELETONIZATION

In this section, we review preliminaries which are useful in understanding the strong recursive skeletonization algorithm. First, we discuss Gaussian elimination and block elimination matrices in Section 3.1. Then, we discuss interpolative decompositions (ID) for low rank compression in Section 3.2, which use a subset of the rows or columns of the original matrix as a basis. Section 3.3 describes how the interpolative decomposition can be used to represent off-diagonal blocks in a rank-structured  $\mathbf{A}$  to efficiently compute a direct solver  $\mathbf{A}^{-1}$ .

**3.1. Gaussian elimination and block elimination matrices.** Consider a matrix of the form

$$\mathbf{A} = \begin{pmatrix} \mathbf{A}_{11} & \mathbf{A}_{12} & \mathbf{0} \\ \mathbf{A}_{21} & \mathbf{A}_{22} & \mathbf{A}_{23} \\ \mathbf{0} & \mathbf{A}_{32} & \mathbf{A}_{33} \end{pmatrix}.$$

If  $\mathbf{A}_{11}$  is non-singular, we can “decouple” it from the other blocks via one step of *block Gaussian elimination*. We express this mathematically through a factorization

$$(22) \quad \mathbf{A} = \begin{pmatrix} \mathbf{A}_{11} & \mathbf{A}_{12} & \mathbf{0} \\ \mathbf{A}_{21} & \mathbf{A}_{22} & \mathbf{A}_{23} \\ \mathbf{0} & \mathbf{A}_{32} & \mathbf{A}_{33} \end{pmatrix} = \mathbf{L} \begin{pmatrix} \mathbf{A}_{11} & \mathbf{0} & \mathbf{0} \\ \mathbf{0} & \mathbf{S}_{22} & \mathbf{A}_{23} \\ \mathbf{0} & \mathbf{A}_{32} & \mathbf{A}_{33} \end{pmatrix} \mathbf{U}$$

where  $\mathbf{L}$  and  $\mathbf{U}$  are “block elimination matrices” of the form

$$(23) \quad \mathbf{L} = \begin{pmatrix} \mathbf{I} & \mathbf{0} & \mathbf{0} \\ \mathbf{A}_{21}\mathbf{A}_{11}^{-1} & \mathbf{I} & \mathbf{0} \\ \mathbf{0} & \mathbf{0} & \mathbf{I} \end{pmatrix} \quad \text{and} \quad \mathbf{U} = \begin{pmatrix} \mathbf{I} & \mathbf{A}_{11}^{-1}\mathbf{A}_{12} & \mathbf{0} \\ \mathbf{0} & \mathbf{I} & \mathbf{0} \\ \mathbf{0} & \mathbf{0} & \mathbf{I} \end{pmatrix},$$

and where  $\mathbf{S}_{22}$  is the “Schur complement”

$$\mathbf{S}_{22} = \mathbf{A}_{22} - \mathbf{A}_{21}\mathbf{A}_{11}^{-1}\mathbf{A}_{12}.$$

For future reference, let us introduce a function  $\mathbf{elim}$  that builds the elimination matrices. To be precise,

$$\mathbf{elim}(\mathbf{B}, I, J, n)$$

is the  $n \times n$  identity matrix, except that the matrix  $\mathbf{B}$  has been inserted in the block identified by the index vector  $I$  and  $J$ . In other words, in (23),

$$\mathbf{L} = \mathbf{elim}(\mathbf{A}_{21}\mathbf{A}_{11}^{-1}, I_2, I_1, n) \quad \text{and} \quad \mathbf{U} = \mathbf{elim}(\mathbf{A}_{11}^{-1}\mathbf{A}_{12}, I_1, I_2, n).$$

Note that block-elimination matrices of the form  $\mathbf{elim}$  are simple to invert by toggling the sign of the off-diagonal block, e.g.

$$\mathbf{L}^{-1} = \mathbf{elim}(-\mathbf{A}_{21}\mathbf{A}_{11}^{-1}, I_2, I_1, n)$$

**Remark 1.** When  $\mathbf{A}$  is symmetric and positive definite (spd), it is preferable to compute its Cholesky factorization. We would then first factorize the  $\mathbf{A}_{11}$  block as

$$\mathbf{A}_{11} = \mathbf{C}_{11}\mathbf{C}_{11}^*$$

where  $\mathbf{C}_{11}$  is lower triangular. Then instead of (22), we would form the triangular factorization

$$\begin{pmatrix} \mathbf{A}_{11} & \mathbf{A}_{12} & \mathbf{0} \\ \mathbf{A}_{21} & \mathbf{A}_{22} & \mathbf{A}_{23} \\ \mathbf{0} & \mathbf{A}_{32} & \mathbf{A}_{33} \end{pmatrix} = \begin{pmatrix} \mathbf{C}_{11} & \mathbf{0} & \mathbf{0} \\ \mathbf{A}_{21}\mathbf{C}_{11}^{-*} & \mathbf{I} & \mathbf{0} \\ \mathbf{0} & \mathbf{0} & \mathbf{I} \end{pmatrix} \begin{pmatrix} \mathbf{I} & \mathbf{0} & \mathbf{0} \\ \mathbf{0} & \mathbf{S}_{22} & \mathbf{A}_{23} \\ \mathbf{0} & \mathbf{A}_{32} & \mathbf{A}_{33} \end{pmatrix} \begin{pmatrix} \mathbf{C}_{11}^* & \mathbf{C}_{11}^{-1}\mathbf{A}_{12} & \mathbf{0} \\ \mathbf{0} & \mathbf{I} & \mathbf{0} \\ \mathbf{0} & \mathbf{0} & \mathbf{I} \end{pmatrix}.$$

When  $\mathbf{A}$  is not spd, one could form analogous triangular factorizations using either the (partially pivoted) LU decomposition of  $\mathbf{A}_{11}$ , or potentially an LDL factorization. In this manuscript, we will focus on block diagonal factorizations, but all techniques described can easily be adapted to form triangular factorizations instead.

**3.2. The interpolatory decomposition.** Let  $\mathbf{B}$  be an  $m \times n$  matrix of rank  $k$ . The *interpolatory decomposition (ID)* of  $\mathbf{B}$  is a low rank factorization where a subset of the columns/rows are used to span its column/row space. For instance, in the *column ID*, we pick a set of  $k$  linearly independent columns identified through the “skeleton” index vector  $J_s$ , and collect the remaining indices in the “residual” index vector  $J_r$ , and set

$$J = [J_r, J_s], \quad \mathbf{B}_r = \mathbf{B}(:, J_r), \quad \mathbf{B}_s = \mathbf{B}(:, J_s),$$

Since  $\mathbf{B}$  has rank  $k$ , there exists a matrix  $\mathbf{T}_{sr}$  of size  $k \times (n - k)$  such that

$$\mathbf{B}_r = \mathbf{B}_s \mathbf{T}_{sr}.$$

This allows us to factor the matrix  $\mathbf{B}$  as

$$(24) \quad \mathbf{B}(:, J) = (\mathbf{B}_r, \mathbf{B}_s) = (\mathbf{B}_s \mathbf{T}_{sr}, \mathbf{B}_s) = (\mathbf{0}, \mathbf{B}_s) \begin{pmatrix} \mathbf{I} & \mathbf{0} \\ \mathbf{T}_{sr} & \mathbf{I} \end{pmatrix}.$$

Interpolatory decompositions can also be computed of matrices that are only of approximate low rank. The errors induced can in theory be significantly larger than those resulting from the optimal low rank decomposition obtained by truncating a singular value decomposition. However, in practice the error tends to be modest as long as the singular values of the input matrix decay at a decent rate. For numerical stability, we would like the matrix  $\begin{pmatrix} \mathbf{I} & \mathbf{0} \\ \mathbf{T}_{sr} & \mathbf{I} \end{pmatrix}$  to be as well-conditioned as possible, but in practice tends to mean that we want the entries of  $\mathbf{T}_{sr}$  to be small. It has been



demonstrated that it is always possible to pick the set  $J_s$  so that every entry of  $\mathbf{T}_{sr}$  has modulus bounded by one, and practical algorithms that ensure that the entries are of modest size are known. See [5] for a detailed discussion of different algorithms for computing the ID in practice.

For completeness, let us also describe the *row ID*, where a set of linearly independent rows of  $\mathbf{B}$  would be identified by an index vector  $I_s$ . Collecting the remaining row indices in the index vector  $I_r$ , we then get the factorization

$$\mathbf{B}([I_r, I_s], :) = \begin{pmatrix} \mathbf{I} & \mathbf{T}_{rs} \\ \mathbf{0} & \mathbf{I} \end{pmatrix} \begin{pmatrix} \mathbf{0} \\ \mathbf{B}_s \end{pmatrix},$$

where  $\mathbf{B}_{rs}$  is the  $(m - k) \times k$  matrix such that  $\mathbf{B}(I_r, :) = \mathbf{T}_{rs} \mathbf{B}(I_s, :)$ .

**3.3. Classical skeletonization (weak admissibility).** We in this section describe how the interpolatory decomposition that we introduced in Section 3.2 can be used to exploit rank deficiencies in off-diagonal blocks to map a given linear system to another “equivalent one” one with a smaller coefficient matrix. The technique described has previously been published as a fast direct solver for boundary integral equations, and is now widely known as “recursive skeletonization” [24, 11, 23, 6, 7]. It is based on “weak admissibility”, and forms the basis for the more complex algorithm based on strong admissibility that is the main focus of this manuscript.

As a model problem, let us consider a matrix  $\mathbf{A}$  that has been partitioned into  $2 \times 2$  blocks as

$$(25) \quad \mathbf{A} = \left( \begin{array}{c|c} \mathbf{A}_{bb} & \mathbf{A}_{ab} \\ \hline \mathbf{A}_{fb} & \mathbf{A}_{ff} \end{array} \right),$$

where the off-diagonal blocks  $\mathbf{A}_{fb}$  and  $\mathbf{A}_{bf}$  each have low rank. Let  $k$  denote the rank of these blocks, and let  $m$  and  $n$  represent the dimensions of the blocks  $\mathbf{A}_{bb}$  and  $\mathbf{A}_{ff}$ , respectively. We will construct block elimination matrices that map  $\mathbf{A}$  to a block diagonal matrix where one block has size  $(m - k) \times (m - k)$ , and other has size  $(k + n) \times (k + n)$ . Let  $I_b$  and  $I_f$  denote index vectors that identify the blocks, so that

$$(1 : n) = I_b \cup I_f.$$

(For now, our discussion is one purely of linear algebra, but we use notation that will serve us well when applying these ideas to solve potential problems in Section 4.) The first step of the factorization process is to form the row ID of  $\mathbf{A}_{af}$  and the column ID of  $\mathbf{A}_{fa}$  to obtain factorizations

$$(26) \quad \mathbf{A}_{bf}([I_r, I_s], :) = \begin{pmatrix} \mathbf{A}_{rf} \\ \mathbf{A}_{sf} \end{pmatrix} = \begin{pmatrix} \mathbf{T}_{rs} \mathbf{A}_{sf} \\ \mathbf{A}_{sf} \end{pmatrix}$$

and

$$(27) \quad \mathbf{A}_{fb}(:, [J_r, J_s]) = [\mathbf{A}_{fr}, \mathbf{A}_{fs}] = [\mathbf{A}_{fs} \mathbf{T}_{sr}, \mathbf{A}_{fs}].$$

Let us reorder the indices within the current box to have the residual indices go first:

$$I = [I_r, I_s, I_f], \quad \text{and} \quad J = [J_r, J_s, I_f].$$

This results in the tessellation

$$(28) \quad \mathbf{A}(I, J) = \left( \begin{array}{cc|c} \mathbf{A}_{rr} & \mathbf{A}_{rs} & \mathbf{A}_{rf} \\ \mathbf{A}_{sr} & \mathbf{A}_{ss} & \mathbf{A}_{sf} \\ \hline \mathbf{A}_{fr} & \mathbf{A}_{fs} & \mathbf{A}_{ff} \end{array} \right) = \left( \begin{array}{cc|c} \mathbf{A}_{rr} & \mathbf{A}_{rs} & \mathbf{T}_{rs} \mathbf{A}_{sf} \\ \mathbf{A}_{sr} & \mathbf{A}_{ss} & \mathbf{A}_{sf} \\ \hline \mathbf{A}_{fs} \mathbf{T}_{sr} & \mathbf{A}_{fs} & \mathbf{A}_{ff} \end{array} \right).$$

Next, we factorize the matrix to introduce zero blocks in the “fr” and “rf” locations:

$$(29) \quad \mathbf{A}(I, J) = \left( \begin{array}{cc|c} \mathbf{I} & \mathbf{T}_{rs} & \mathbf{0} \\ \mathbf{0} & \mathbf{I} & \mathbf{0} \\ \hline \mathbf{0} & \mathbf{0} & \mathbf{I} \end{array} \right) \left( \begin{array}{cc|c} \mathbf{X}_{rr} & \mathbf{X}_{rs} & \mathbf{0} \\ \mathbf{X}_{sr} & \mathbf{A}_{ss} & \mathbf{A}_{sf} \\ \hline \mathbf{0} & \mathbf{A}_{fs} & \mathbf{A}_{ff} \end{array} \right) \left( \begin{array}{cc|c} \mathbf{I} & \mathbf{0} & \mathbf{0} \\ \mathbf{T}_{sr} & \mathbf{I} & \mathbf{0} \\ \hline \mathbf{0} & \mathbf{0} & \mathbf{I} \end{array} \right).$$

Recognizing that the outside factors in (29) are both block elimination matrices, we define

$$\mathbf{E} := \text{elim}(\mathbf{T}_{rs}, I_r, I_s, n) \quad \text{and} \quad \mathbf{F} := \text{elim}(\mathbf{T}_{sr}, J_s, J_r, n).$$

so that we can rewrite (29) as

$$(30) \quad \mathbf{E} \left( \begin{array}{cc|c} \mathbf{X}_{\text{rr}} & \mathbf{X}_{\text{rs}} & \mathbf{0} \\ \mathbf{X}_{\text{sr}} & \mathbf{A}_{\text{ss}} & \mathbf{A}_{\text{sf}} \\ \mathbf{0} & \mathbf{A}_{\text{fs}} & \mathbf{A}_{\text{ff}} \end{array} \right) \mathbf{F}.$$

We next perform one step of block Gaussian elimination to decouple  $\mathbf{X}_{\text{rr}}$ , so that

$$\mathbf{A}(I, J) = \mathbf{E}\mathbf{L} \left( \begin{array}{cc|c} \mathbf{X}_{\text{rr}} & \mathbf{0} & \mathbf{0} \\ \mathbf{0} & \mathbf{X}_{\text{ss}} & \mathbf{A}_{\text{sf}} \\ \mathbf{0} & \mathbf{A}_{\text{fs}} & \mathbf{A}_{\text{ff}} \end{array} \right) \mathbf{U}\mathbf{F},$$

where  $\mathbf{L}$  and  $\mathbf{U}$  are the block elimination matrices

$$\mathbf{L} = \text{elim}(\mathbf{X}_{\text{sr}}\mathbf{X}_{\text{rr}}^{-1}, I_s, I_r, n) \quad \text{and} \quad \mathbf{U} = \text{elim}(\mathbf{X}_{\text{rr}}^{-1}\mathbf{X}_{\text{rs}}, J_r, J_s, n).$$

#### 4. STRONG RECURSIVE SKELETONIZATION

In this section, we review the strong recursive skeletonization (SRS) algorithm of [25] that is used to compute an invertible factorization of a dense matrix involving a kernel matrix whose kernel represents physical interactions between a set of points in two or three dimensions. The decomposition is related to classical skeletonization as introduced in Section 3.3, however, the skeletonization is performed with “strong admissibility” condition, where only well-separated boxes are compressed as low-rank.

First, we discuss a hierarchical tree data structure which gives useful terminology for discussing the algorithm. In Section 4.2, we discuss the strong recursive skeletonization procedure for a single box of the tree, and in Section 4.3, we describe how the algorithm can be applied recursively in a traversal of the tree. Section 4.4 discusses how the factorization can be computed efficiently in circumstances where matrix entries of  $\mathbf{A}$  can be accessed easily, setting the stage for computing the factorization in the black-box setting.

In the introduction of the ideas, we focus on the simple quasi-one dimensional domain of Figure 3, though the ideas are directly applicable to more complicated domains, as shown in Figure 6.

**4.1. Hierarchical tree structure.** SRS relies on a hierarchical partitioning of given points  $\{\mathbf{x}_j\}_{j=1}^N$  into an quad-tree or oct-tree. For the purposes of this discussion, we restrict our attention to uniform (e.g. fully populated) trees. Formally, we define a tree  $\mathcal{T}$ , in which each box  $b$  is associated with a subset of the given points. Initially, all points belong to the root node. Letting  $d$  denote the dimension, we split the root node into  $2^d$  children nodes, and then split each child again until the size of each node is below some given threshold  $m$ . We refer to a node with children as a parent node, and a node with no children as a leaf node. The depth of a node is defined as its distance from the root node, and level  $\ell$  of the tree is defined as the set of nodes with depth  $\ell$ , so that level 0 consists of only the root node, level 1 consists of the  $2^d$  children of the root node, and so on. The levels of the tree represent successively finer partitions of the points. The depth of the tree is defined as the maximum node depth, denoted by  $L \approx \log_2(N/m)$ . See Figure 6 for a hierarchical decomposition of points into a uniform quadtree.

**4.2. Strong skeletonization for a single box.** Let us consider again the simple model problem on a quasi one dimensional domain in Figure 1 that we introduced in Section 2, where  $\mathbf{A}$  is given by the evaluation of (1) on a set of points  $\{\mathbf{x}_i\}_{i=1}^N$ . Consider the tessellating the given points of Figure 3(a) into boxes 8,  $\dots$ , 15 as shown in Figure 3(b). The objective, in this section, is to describe the process of diagonalizing the interactions between a target box  $b$  and the rest of the points. Once this machinery is in place, the procedure can be applied successively to all boxes on a level.

Consider the target box 8, for concreteness. First, we would like to compress the interactions between box  $b$  and its far field. To this end, we split the set of points into three sets: The box itself which contains all points in the box to be compressed (box 8 in this case), the “near field set” which

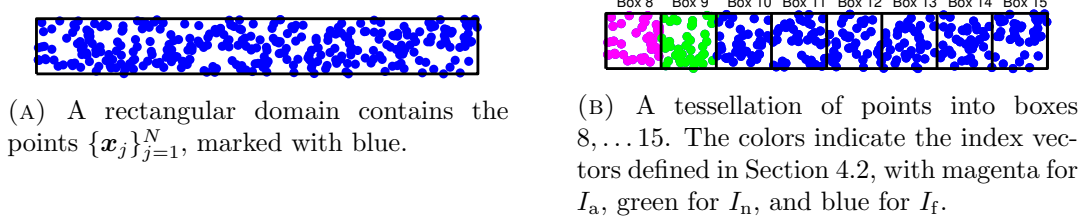


FIGURE 3

contains points in boxes directly adjacent to the active box (box 9 in this case), and the “far field set” which contains everything else (boxes 10 through 15 in this case). These sets are identified through three index vectors:

- $I_b$  The “target box”. (While compressing box 8,  $I_b = I_8$ .)
- $I_n$  The “near field indices”. (While compressing box 8,  $I_n = I_9$ .)
- $I_f$  The “far field indices”. (While compressing box 8,  $I_f = [I_{10}, I_{11}, \dots, I_{15}]$ .)

Figure 3(b) illustrates these definitions. Setting  $I = J = [I_b, I_n, I_f]$ , we now obtain a partition of  $\mathbf{A}$  into the blocks

$$(31) \quad \mathbf{A}(I, J) = \left( \begin{array}{c|cc} \mathbf{A}_{bb} & \mathbf{A}_{bn} & \mathbf{A}_{bf} \\ \mathbf{A}_{nb} & \mathbf{A}_{nn} & \mathbf{A}_{nf} \\ \mathbf{A}_{fb} & \mathbf{A}_{fn} & \mathbf{A}_{ff} \end{array} \right).$$

(Comparing (31) to the tessellation (32) that is used in classical skeletonization, we see that the near field has been added. The purpose is to reduce the numerical ranks that arise.) We now invoke the well-known fact from the literature on fast summation schemes that all interactions between the active box and its far-field has low numerical rank. (To be precise, the rank is bounded by  $O(\log(1/\varepsilon))$  where  $\varepsilon$  is the requested precision. This bound is independent of how many points are actually in the box.) Linear algebraically, this means that  $\mathbf{A}_{bf}$  and  $\mathbf{A}_{fb}$  are both of numerically low rank. We form the row and the column IDs, respectively, cf. (26) and (27),

$$(32) \quad \mathbf{A}_{bf}([I_r, I_s], :) = \begin{pmatrix} \mathbf{A}_{rf} \\ \mathbf{A}_{sf} \end{pmatrix} = \begin{pmatrix} \mathbf{T}_{rs} \mathbf{A}_{sf} \\ \mathbf{A}_{sf} \end{pmatrix}$$

and

$$(33) \quad \mathbf{A}_{fb}(:, [J_r, J_s]) = [\mathbf{A}_{fr}, \mathbf{A}_{fs}] = [\mathbf{A}_{fs} \mathbf{T}_{sr}, \mathbf{A}_{fs}].$$

These factorizations partition the nodes in  $I_b$  into a set of “skeleton nodes” that represent all interactions between the box and the outside world, and a set of “residual nodes” that we will decouple from the rest of the system. To keep track of this, we update  $I$  and  $J$  to put the residual nodes first:

$$I = [I_r, I_s, I_n, I_f], \quad \text{and} \quad J = [J_r, J_s, I_n, I_f].$$

The corresponding tessellation of  $\mathbf{A}$  becomes, cf. (28),

$$(34) \quad \mathbf{A}(I, J) = \left( \begin{array}{cc|cc} \mathbf{A}_{rr} & \mathbf{A}_{rs} & \mathbf{A}_{rn} & \mathbf{A}_{rf} \\ \mathbf{A}_{sr} & \mathbf{A}_{ss} & \mathbf{A}_{sn} & \mathbf{A}_{sf} \\ \mathbf{A}_{nr} & \mathbf{A}_{ns} & \mathbf{A}_{nn} & \mathbf{A}_{nf} \\ \mathbf{A}_{fr} & \mathbf{A}_{fs} & \mathbf{A}_{fn} & \mathbf{A}_{ff} \end{array} \right) = \left( \begin{array}{cc|cc} \mathbf{A}_{rr} & \mathbf{A}_{rs} & \mathbf{A}_{rn} & \mathbf{T}_{rs} \mathbf{A}_{sf} \\ \mathbf{A}_{sr} & \mathbf{A}_{ss} & \mathbf{A}_{sn} & \mathbf{A}_{sf} \\ \mathbf{A}_{nr} & \mathbf{A}_{ns} & \mathbf{A}_{nn} & \mathbf{A}_{nf} \\ \mathbf{A}_{fs} \mathbf{T}_{sr} & \mathbf{A}_{fs} & \mathbf{A}_{fn} & \mathbf{A}_{ff} \end{array} \right)$$

Eliminating the “fr” and the “rf” blocks from (34), we next get

$$(35) \quad \mathbf{A}(I, J) = \mathbf{E} \left( \begin{array}{cc|cc} \mathbf{X}_{rr} & \mathbf{X}_{rs} & \mathbf{X}_{rn} & \mathbf{0} \\ \mathbf{X}_{sr} & \mathbf{A}_{ss} & \mathbf{A}_{sn} & \mathbf{A}_{sf} \\ \mathbf{X}_{nr} & \mathbf{A}_{ns} & \mathbf{A}_{nn} & \mathbf{A}_{nf} \\ \mathbf{0} & \mathbf{A}_{fs} & \mathbf{A}_{fn} & \mathbf{A}_{ff} \end{array} \right) \mathbf{F}$$

where

$$\mathbf{E} = \text{elim}(\mathbf{T}_{rs}, I_r, I_s, n) \quad \text{and} \quad \mathbf{F} = \text{elim}(\mathbf{T}_{sr}, J_s, J_r, n).$$

Then block Gaussian elimination yields the factorization

$$(36) \quad \mathbf{A}(I, J) = \mathbf{E}\mathbf{L} \left( \begin{array}{cc|cc} \mathbf{X}_{rr} & \mathbf{0} & \mathbf{0} & \mathbf{0} \\ \mathbf{0} & \mathbf{X}_{ss} & \mathbf{X}_{sn} & \mathbf{A}_{sf} \\ \hline \mathbf{0} & \mathbf{X}_{ns} & \mathbf{X}_{nn} & \mathbf{A}_{nf} \\ \mathbf{0} & \mathbf{A}_{fs} & \mathbf{A}_{fn} & \mathbf{A}_{ff} \end{array} \right) \mathbf{U}\mathbf{F}$$

where  $\mathbf{L}$  and  $\mathbf{U}$  are the block elimination matrices

$$(37) \quad \mathbf{L} = \text{elim}(\mathbf{X}_{sr}\mathbf{X}_{rr}^{-1}, I_s, I_r, n) \quad \text{and} \quad \mathbf{U} = \text{elim}(\mathbf{X}_{rr}^{-1}\mathbf{X}_{rs}, J_r, J_s, n).$$

The equation (36) successfully decouples the residual nodes of target box  $b$  from the rest of the problem. Alternatively, the system can be written as

$$(38) \quad \tilde{\mathbf{A}} = \mathbf{V}^{-1}\mathbf{A}(I, J)\mathbf{W}^{-1}, \quad \mathbf{V} := \mathbf{E}\mathbf{L}, \quad \mathbf{W} := \mathbf{U}\mathbf{F}$$

where the matrices  $\mathbf{V}$  and  $\mathbf{W}$  are defined as the left and right diagonalization operators, respectively, and the matrix  $\tilde{\mathbf{A}}$  is written explicitly in the equation (36). The redundant nodes of the target box are decoupled in equation (36), and the algorithm proceeds by repeating a similar procedure to the other boxes of the tree, but now for the modified system  $\tilde{\mathbf{A}}$ .

**4.3. Recursive Algorithm.** In the previous section, we described the procedure for decoupling the redundant nodes of a target box from the rest of the system. Now, we describe how this procedure can be applied successively to all boxes on a level. Consider again the simple model of a quasi-one dimensional geometry in Figure 1. For target box 8, the left and right diagonalization operators  $\mathbf{V}_8$  and  $\mathbf{W}_8$  have the form described in Section 4.2. Applying these operators to the appropriate permutation of  $\mathbf{A}$  yields the matrix  $\tilde{\mathbf{A}}$  defined in (38). For the sparsity pattern of  $\tilde{\mathbf{A}}$ , see the leftmost panel of Figure 4, where the modified entries of  $\tilde{\mathbf{A}}$  are highlighted in red. The procedure can be repeated for target box 9 by computing left and right diagonalization operators  $\mathbf{V}_9$  and  $\mathbf{W}_9$ . Note that instead of computing skeletons for the original matrix  $\mathbf{A}$  as in equation (34), we instead need to compute skeletons which sparsify the modified matrix  $\tilde{\mathbf{A}}$ . Applying these techniques to the boxes 8,  $\dots$ , 15 on Level 3 successively, we can compute a factorization, which (for an appropriate permutation) has the following form

$$(39) \quad \left( \begin{array}{cccc} \tilde{\mathbf{A}}_{r8} & & & \\ & \tilde{\mathbf{A}}_{r9} & & \\ & & \ddots & \\ & & & \tilde{\mathbf{A}}_{r15} \\ & & & & \tilde{\mathbf{A}}_{[s8, \dots, s15]} \end{array} \right) = \mathbf{V}_{15}^{-1} \dots \mathbf{V}_8^{-1} \mathbf{A} \mathbf{W}_{15}^{-1} \dots \mathbf{W}_8^{-1},$$

where  $\tilde{\mathbf{A}}$  is a matrix of modified interactions. The redundant nodes  $I_r$  for every box 8,  $\dots$ , 15 are decoupled from the rest of the system. The remaining nodes  $I_s$  of skeleton nodes for every box interact densely in the dense block  $\tilde{\mathbf{A}}_{[s8, \dots, s15]}$ . In the process of computing the single-level factorization (39), the modified matrix of decoupled interactions need to be stored and updated. See Figure 4 for the sparsity pattern of decoupled interactions at various stages of computing the single-level factorization (39). Typically, strong recursive skeletonization is applied in circumstances where entries of  $\mathbf{A}$  can be accessed in  $\mathcal{O}(1)$  time, and the entire matrix of decoupled interactions does not need to be stored explicitly. Then, only the modified entries shown in red of Figure 4 need to be stored at every stage of the computation.

Since the residual degrees of freedom have been decoupled from the problem in (39), the task that remains is to solve the surviving linear system on the ‘‘skeleton nodes’’. To illustrate the structure of this problem, we show the coefficient matrix after the residual nodes have been dropped in Figure

5(a). For intermediate size problems, it is often possible to directly compute the LU decomposition of the linear system that connects the skeleton nodes, since the ranks tend to be small when strong admissibility is used. However, for large scale problems, there will be too many skeleton nodes surviving. In this case, we can continue the skeletonization process in a multilevel fashion. In order to reintroduce rank deficiencies in the off-diagonal blocks, we merge the boxes by twos to form larger boxes, as shown in 5(b). The idea is now to simply repeat the skeletonization process outlined in Section 4.2. This results in the further sparsified coefficient matrix shown in Figure 5(c).

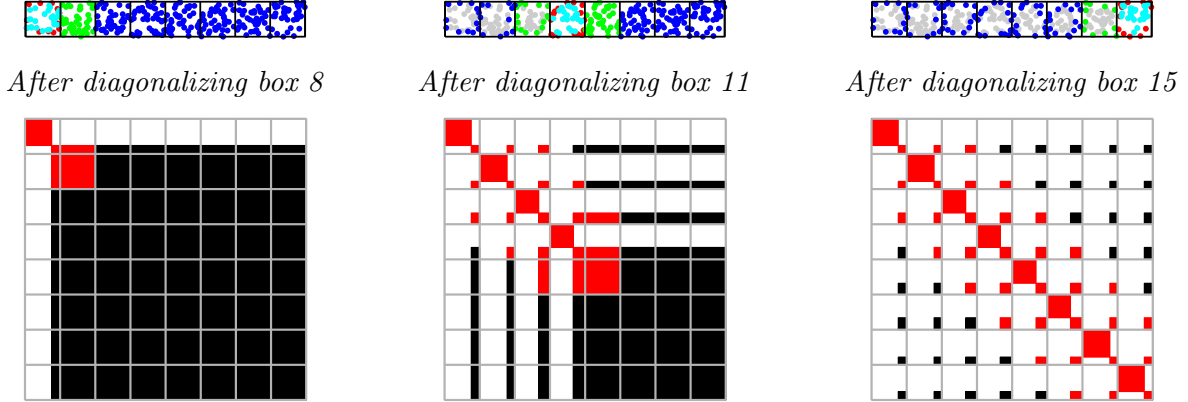


FIGURE 4. Illustration of the combined compression and factorization process described in Section 4.2. *Upper row:* The computational domain after steps 1, 4, and 8. The nodes are colored so that  $I_s$  is red,  $I_r$  is cyan,  $I_n$  is green, and  $I_f$  is blue. (The gray nodes mark points that were identified as “residual” nodes in the previous steps. These points have dropped out of the computation and play no active role.) *Lower row:* The sparsity pattern of the matrix  $\tilde{\mathbf{A}}$  after the residual nodes in Box 8/11/15 have been decoupled. White blocks are zeros, red blocks are entries that got modified, and black blocks are entries that have not been modified.

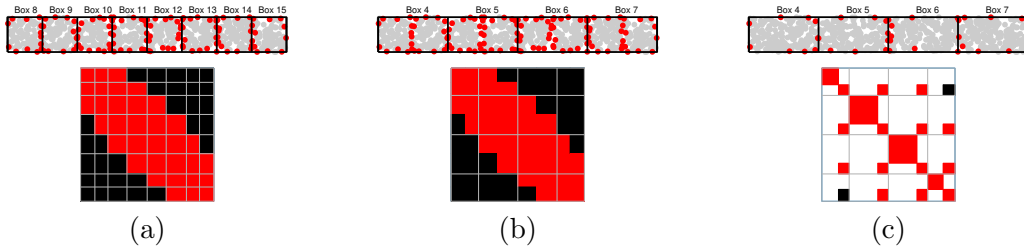


FIGURE 5. Illustration of the merging of boxes described in Section 4.3. (a) On top, the points remaining active after compression of the first level has completed. Below, the corresponding coefficient matrix, with entries that have been modified shown in red. (b) Boxes on the finest level have been merged by pairs to create larger boxes and reintroduce rank deficiencies in the off-diagonal blocks. (c) The geometry and the coefficient matrix after compression at the coarser level has completed.

We will shortly formalize the description of the recursive skeletonization process, but let us first briefly show what changes occur when the domain is “truly” two dimensional, as in Figure 6(a). It is now natural to organize the domain into a quadtree of boxes, rather than a binary tree, as shown in Figures 6(b) and 6(c). Other than that, the scheme proceeds just as it does for the quasi one

dimensional example we discussed earlier. After all boxes at the finest level have been compressed, the remaining skeleton points are shown on top in Figure 7(a) in red, while the residual points are shown in gray. The matrix of interactions between the skeleton points is shown below. Observe that there are now many more updated (red) boxes than there were for the quasi one dimensional domain (as many as 25 in some rows). In order to reintroduce rank deficiencies in the off-diagonal blocks, we now merge boxes by sets of four to yield level 2, as illustrated in Figure 7(b). Once compression has completed at level 2, very few points remain as skeleton nodes, as we see on top in Figure 7(c), with the very sparse coefficient matrix shown below.

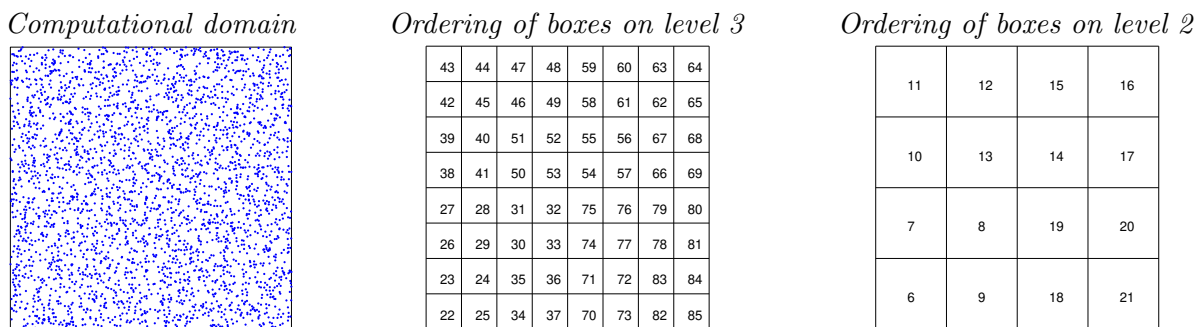


FIGURE 6. The square computational domain described in Section 4.1. (a) The original domain, with the points  $\{\mathbf{x}_i\}_{i=1}^N$  shown in blue. (b) The boxes at the finest level. (c) The merged boxes at the next coarser level.

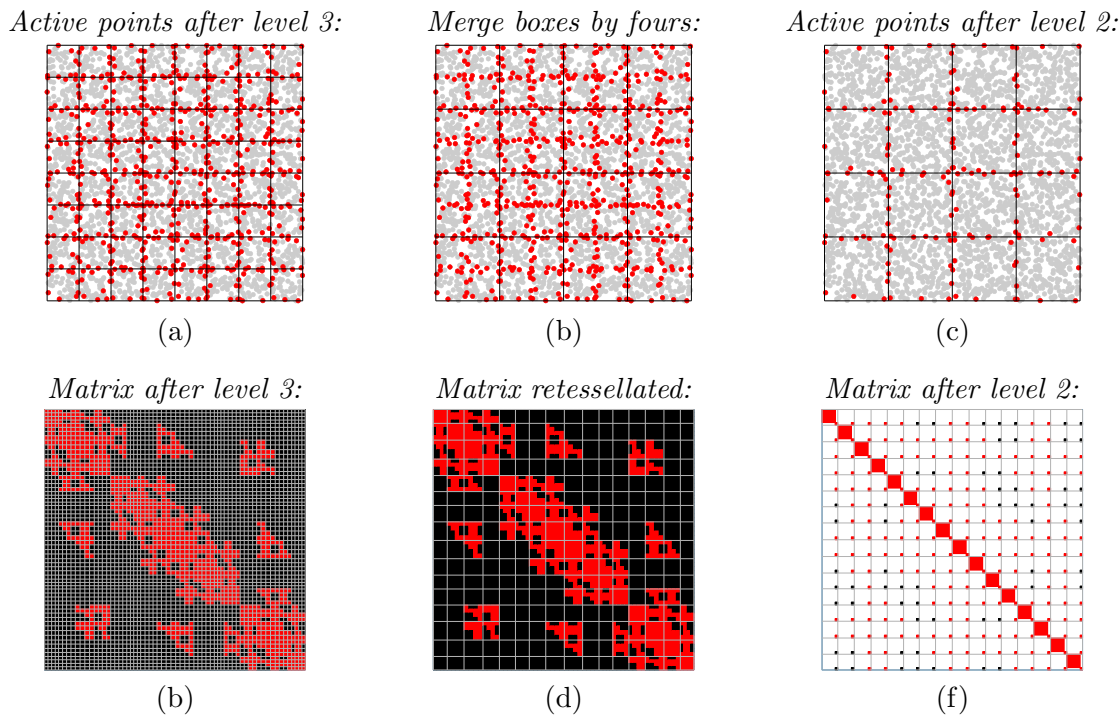


FIGURE 7. The analog of Figure 5 when the computational domain is the box shown in Figure 1. Observe that many more blocks get updated for a true two-dimensional domain — up to 25 boxes per row need to be explicitly stored.

To formalize the description of SRS, consider that the boxes are diagonalized in an upward traversal through the tree in order  $1, \dots, n$ . Then the decomposition takes the form

$$(40) \quad \tilde{\mathbf{A}}_{\text{diag}} := \begin{pmatrix} \tilde{\mathbf{A}}_{r_1} & & & & \\ & \tilde{\mathbf{A}}_{r_2} & & & \\ & & \ddots & & \\ & & & \tilde{\mathbf{A}}_{r_n} & \\ & & & & \tilde{\mathbf{A}}_{[S]} \end{pmatrix} = \mathbf{V}_1^{-1} \dots \mathbf{V}_n^{-1} \mathbf{A} \mathbf{W}_n^{-1} \dots \mathbf{W}_1^{-1},$$

where  $[S]$  is the set of all remaining skeleton nodes at the time of terminating the algorithm (typically on level 2 of the tree). Because  $\tilde{\mathbf{A}}_{\text{diag}}$  is block-diagonal, it is easy to invert. The factorization (40) can also be used for a sparse factorization of  $\mathbf{A}$ . In the next section, we discuss techniques which allow for the efficient calculation of elimination matrices  $\mathbf{E}$  and  $\mathbf{F}$  of Section 4.2 in the setting of boundary integral equations.

**4.4. How to compress the far-field interactions.** The aim is to compress the two off-diagonal blocks  $\mathbf{A}_{b,f}$  and  $\mathbf{A}_{f,b}$  using the column ID. Notice that the computational cost would be  $\mathcal{O}(N)$  if the full matrix is formed, which turns out to be unnecessary, particularly when  $\mathbf{A}$  arises from the discretization of a boundary integral equation.

The proxy method introduces points  $\{\mathbf{x}_i^{(\text{proxy})}\}_{i=1}^{n_p}$  which replicate the effect of far-field points  $I_f$ . Instead of using the matrix  $\mathbf{A}_{b,f}$ , a smaller matrix with  $\mathcal{O}(1)$  rows and columns is formed and compressed

$$(41) \quad \mathbf{A}_{\text{proxy},b} \quad \text{where } (\mathbf{A}_{\text{proxy},b})_{i,j} = k(\mathbf{x}_i^{(\text{proxy})}, \mathbf{x}[I_{b_j}]).$$

With the appropriate choice of proxy surface, the matrix  $\mathbf{A}_{\text{proxy},b}$  spans the row space of  $\mathbf{A}_{f,b}$ , and likewise,  $\mathbf{A}_{b,\text{proxy}}$  spans the column space of  $\mathbf{A}_{b,f}$  for *any* point distribution in the far-field. Therefore, the indices  $I_b = I_r \cup I_s$  and interpolative matrix  $\tilde{\mathbf{T}}$  computed by forming and factorizing the matrix (41) will satisfy (33). Because the matrix  $\tilde{\mathbf{A}}$  of diagonalized interactions does modify entries of  $\mathbf{A}$ , the proxy surface needs to be placed appropriately to compute the SRS factorization; this is discussed in further detail in [25, 27].

## 5. RANDOMIZED STRONG RECURSIVE SKELETONIZATION

In this section, we describe computing the SRS factorization described in Section 4 in the black-box setting where the matrix  $\mathbf{A}$  is only accessed through its action on vectors. The algorithm relies on the randomized sampling machinery first introduced in Section 2. Recall that our setting is the following

$$(42) \quad \begin{matrix} \mathbf{Y} \\ N \times p \end{matrix} = \begin{matrix} \mathbf{A} \\ N \times N \end{matrix} \begin{matrix} \boldsymbol{\Omega} \\ N \times p \end{matrix}, \quad \begin{matrix} \mathbf{Z} \\ N \times p \end{matrix} = \begin{matrix} \mathbf{A}^* \\ N \times N \end{matrix} \begin{matrix} \boldsymbol{\Psi} \\ N \times p \end{matrix}, \quad \boldsymbol{\Omega}, \boldsymbol{\Psi} \sim \mathcal{N}(\mathbf{0}, \mathbf{I})$$

where the matrix  $\mathbf{A}$  and its adjoint are sketched with Gaussian random matrices.

As in our description of SRS, we first describe the process of diagonalizing the interactions of a target box  $b$  with respect to the rest of the problem. Recall the notation used in Section 4.2 for a target box  $I_b$ , its near-field indices  $I_n$  and its far-field indices  $I_f$ .

In order to compute the skeletonization operators  $\mathbf{E}$  and  $\mathbf{F}$ , we need to compute the column ID of the sketches

$$(43) \quad \begin{matrix} \mathbf{Y}'_b \\ m \times k \end{matrix} = \begin{matrix} \mathbf{A}_{bf} \\ N \times N \end{matrix} \begin{matrix} \boldsymbol{\Omega}_f \\ N \times p \end{matrix}, \quad \begin{matrix} \mathbf{Z}'_b \\ m \times k \end{matrix} = \begin{matrix} \mathbf{A}_{fb}^* \\ N \times N \end{matrix} \begin{matrix} \boldsymbol{\Psi}_f \\ N \times p \end{matrix},$$

respectively. The samples  $\mathbf{Y}$  and  $\mathbf{Z}$  in (42), however, include the contributions of the near field blocks  $I_n$ . The contribution of  $\boldsymbol{\Omega}_n$  and  $\boldsymbol{\Psi}_n$ , however, can be “nullified” using block nullification as

described in Section 2.2 and sketches (43) can be computed as

$$(44) \quad \mathbf{Y}'_b = \underset{m \times k}{\mathbf{Y}_b} \underset{m \times p}{\text{null}}(\underset{p \times k}{\mathbf{\Omega}_n}), \quad \mathbf{Z}'_b = \underset{m \times k}{\mathbf{Z}_b} \underset{m \times p}{\text{null}}(\underset{p \times k}{\mathbf{\Psi}_n}),$$

The sparsified matrix  $\hat{\mathbf{A}} = \mathbf{E}^{-1} \mathbf{A} \mathbf{F}^{-1}$  has decoupled interactions between  $I_r$  and  $I_f$ , and the interactions between  $I_r$  and the rest of the system can be entirely decoupled using block-elimination matrices  $\mathbf{L}, \mathbf{U}$  as defined in 37. Ideally, we would like to extract the modified interactions between  $\mathbf{X}_{r,n}$  and  $\mathbf{X}_{n,r}$  as well as  $\mathbf{X}_{r,s}$  and  $\mathbf{X}_{s,r}$  in equation (35). The samples  $\{\mathbf{Y}, \mathbf{\Omega}, \mathbf{Z}, \mathbf{\Psi}\} \Rightarrow \{\hat{\mathbf{Y}}, \hat{\mathbf{\Omega}}, \hat{\mathbf{Z}}, \hat{\mathbf{\Psi}}\}$  can be updated to instead be samples of  $\hat{\mathbf{A}}$ .

$$(45) \quad \begin{aligned} \hat{\mathbf{Y}} &= \mathbf{E} \mathbf{Y}, & \hat{\mathbf{\Omega}} &= \mathbf{F}^{-1} \mathbf{\Omega} \\ \hat{\mathbf{Z}} &= \mathbf{F}^* \mathbf{Z}, & \hat{\mathbf{\Psi}} &= \mathbf{E}^{-*} \mathbf{\Psi} \end{aligned}$$

Then the modified interactions  $\mathbf{X}_{r,n}$  and  $\mathbf{X}_{n,r}$  can be extracted using block extraction, as discussed in Section 2.3 using the formulas

$$(46) \quad \mathbf{X}_{r,n} = \hat{\mathbf{Y}}_r \hat{\mathbf{\Omega}}_n^\dagger, \quad \mathbf{X}_{n,r}^* = \hat{\mathbf{Z}}_r \hat{\mathbf{\Psi}}_n^\dagger.$$

After computing the block elimination matrices  $\mathbf{L}$  and  $\mathbf{U}$ , the random sketches can again to updated to be instead of the matrix  $\tilde{\mathbf{A}} = \mathbf{L}^{-1} \hat{\mathbf{A}} \mathbf{U}^{-1}$  by updating the sketches  $\{\hat{\mathbf{Y}}, \hat{\mathbf{\Omega}}, \hat{\mathbf{Z}}, \hat{\mathbf{\Psi}}\}$  to produce sketches  $\{\tilde{\mathbf{Y}}, \tilde{\mathbf{\Omega}}, \tilde{\mathbf{Z}}, \tilde{\mathbf{\Psi}}\}$ .

$$(47) \quad \begin{aligned} \tilde{\mathbf{Y}} &= \mathbf{L} \hat{\mathbf{Y}}, & \tilde{\mathbf{\Omega}} &= \mathbf{U}^{-1} \hat{\mathbf{\Omega}} \\ \tilde{\mathbf{Z}} &= \mathbf{U}^* \hat{\mathbf{Z}}, & \tilde{\mathbf{\Psi}} &= \mathbf{L}^{-*} \hat{\mathbf{\Psi}} \end{aligned}$$

After completing this process for a single box, the procedure can be repeated for a sequence of boxes. Over the course of the algorithm, the samples do not need to be redrawn, instead they are updated using the computed factorization at every stage. Because the algorithm is multi-level, compression errors do propagate from one level to the next. To handle this issue, the absolute tolerance for the compression stage is successively relaxed at every level of the computation. The matrix  $\tilde{\mathbf{A}}$  in equation (40) is block-diagonal to some accuracy which may deviate slightly from the desired compression tolerance. To estimate the extent to which our compression is successful for a particular level, we use randomized sampling techniques (e.g. block nullification) to estimate the extent to which  $\tilde{\mathbf{A}}_{r,f}$  and  $\tilde{\mathbf{A}}_{f,r}$  deviate from desired compression tolerance, where in this case  $I_f = (1 : N) \setminus I_r$ , for every box.

## 6. NUMERICAL EXPERIMENTS

In this section, we illustrate the performance of the proposed algorithm. For the example in Section 6.1, we consider a sparse Schur complement, which arises in the context of sparse direct solvers. Sparse Schur complements are a composition of sparse matrix operations; they can be applied fast to vectors, however, matrix entries are challenging to access efficiently.

$N$	number of points
$m$	leaf size of tree
$T_{\text{factorize}}$	time for Algorithm 5
$M$	memory needed for $\mathbf{V}_i$ and $\mathbf{W}_i$ for all boxes
atol	absolute compression tolerance at the leaf level
relerr	relative maximum error (on a subset of points)
errsolve	relative maximum error (on a subset of points)

TABLE 1. Notation for reported numerical results.



The RSRS algorithm is operates on a uniform quad-tree  $\mathcal{T}$  which is partitioned to have at most  $m$  points in the leaf boxes. The user provides a parameter  $\text{atol}$  which dictates the absolute tolerance of compression at the leaf level; the compression rank  $k$  is chosen for each box adaptively. The success of the algorithm is measured by accessing the relative error of the computed factorization, as well as the error in the computed inverse. For the computed invertible factorization  $\mathbf{K} \approx \mathbf{A}$ , we report

$$(48) \quad \text{relerr} = \frac{\|\mathbf{A} - \mathbf{K}\|_2}{\|\mathbf{A}\|_2}, \quad \text{errsolve} = \|\mathbf{I} - \mathbf{K}^{-1}\mathbf{A}\|_2.$$

Typical choices of user parameter  $\text{atol}$  may be  $10^{-5}$  or even as large as  $10^{-2}$ ; the resulting errors (48) in the factorization are often much smaller, as we will demonstrate in the numerical results. Table 1 summarizes the notation used to report the numerical results.

**6.1. 3D Sparse Direct Solvers.** Consider a boundary value problem of the form

$$(49) \quad \begin{cases} -\Delta u(x) = f(x), & x \in \Omega, \\ u(x) = g(x), & x \in \Gamma, \end{cases}$$

where  $\mathcal{A}$  is a second order elliptic differential operator, and  $\Omega$  is a rectangular domain in three dimensions with boundary  $\Gamma$ . Upon discretizing (49) with 2nd order finite differences, one obtains a linear system

$$\mathbf{A}\mathbf{u} = \mathbf{f},$$

involving a sparse coefficient matrix. Sparse direct solvers produce an invertible factorization of  $\mathbf{A}$  by leveraging sparsity, as well as  $\mathcal{H}$ -matrix structure when appropriate [19, ch. 20,21]. Often, it is useful to decompose the domain for the purposes of parallelizing the computation. The typical choice of domain decomposition is a hierarchical quad-tree or oct-tree, but a decomposition into thin slab subdomains is also possible and advantageous for ease of parallelization. This domain decomposition is employed in SlabLU, which is a simplified two-level sparse direct solver [31]. The corresponding domain decomposition is shown in Figure 8.

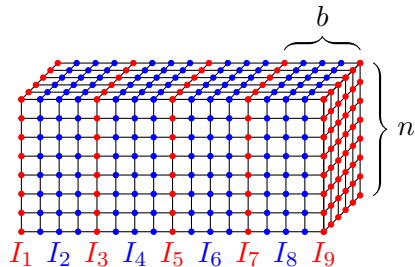


FIGURE 8. Domain decomposition used in SlabLU. The even-numbered nodes correspond to the nodes interior to each subdomain. The odd-numbered nodes correspond to interfaces between slabs. The slab partitioning is chosen so that interactions between slab interiors are zero. The slabs have width of  $b$  points.

To be precise, SlabLU uses a decomposition of the domain into elongated “slab” subdomains of width  $b$ , where the odd-numbered nodes correspond to slab interface nodes and the even-numbered nodes correspond to slab interior nodes. With the slab decomposition, the linear system (6.1) has the block form

$$(50) \quad \begin{bmatrix} \mathbf{A}_{11} & \mathbf{A}_{12} & \mathbf{0} & \mathbf{0} & \mathbf{0} & \dots \\ \mathbf{A}_{21} & \mathbf{A}_{22} & \mathbf{A}_{23} & \mathbf{0} & \mathbf{0} & \dots \\ \mathbf{0} & \mathbf{A}_{32} & \mathbf{A}_{33} & \mathbf{A}_{34} & \mathbf{0} & \dots \\ \mathbf{0} & \mathbf{0} & \mathbf{A}_{43} & \mathbf{A}_{44} & \mathbf{A}_{45} & \dots \\ \vdots & \vdots & \vdots & \vdots & \vdots & \vdots \end{bmatrix} \begin{bmatrix} \mathbf{u}_1 \\ \mathbf{u}_2 \\ \mathbf{u}_3 \\ \mathbf{u}_4 \\ \vdots \end{bmatrix} = \begin{bmatrix} \mathbf{f}_1 \\ \mathbf{f}_2 \\ \mathbf{f}_3 \\ \mathbf{f}_4 \\ \vdots \end{bmatrix}.$$

The system (50) can be factorized by first eliminating the nodes internal to each slab are eliminated in parallel by computing sparse direct factorizations  $\mathbf{A}_{22}^{-1}, \mathbf{A}_{44}^{-1}, \dots$  in parallel. The remaining system

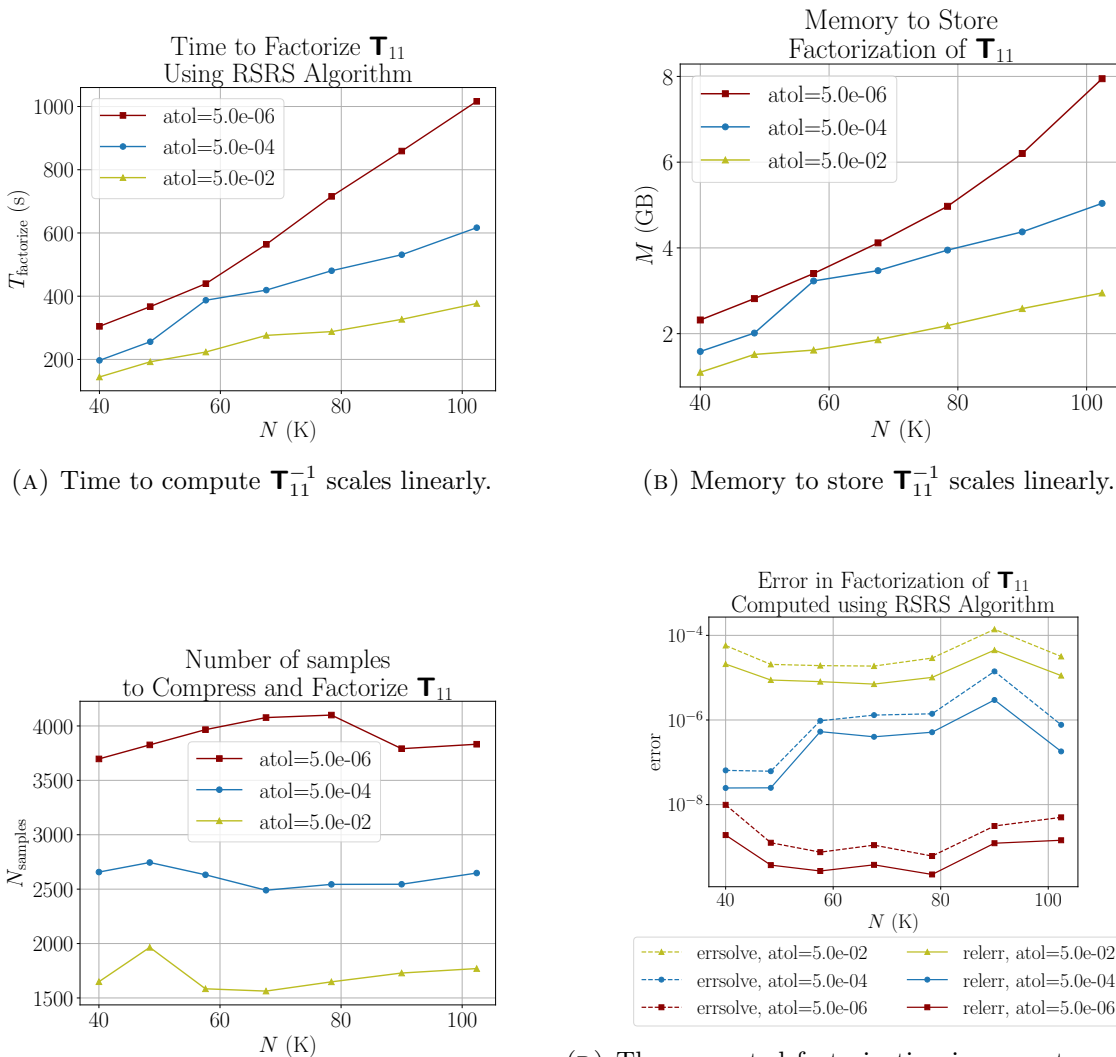
has sparse Schur complements of the form

$$(51) \quad \mathbf{T}_{11} = \mathbf{A}_{11} - \mathbf{A}_{12} \mathbf{A}_{22}^{-1} \mathbf{A}_{21}$$

Owing to sparsity,  $\mathbf{T}_{11}$  and its transpose can be rapidly applied to random vectors

$$(52) \quad \begin{matrix} \mathbf{Y} \\ n^2 \times s \end{matrix} = \begin{matrix} \mathbf{T}_{11} \\ n^2 \times n^2 \end{matrix} \begin{matrix} \boldsymbol{\Omega} \\ n^2 \times s \end{matrix}, \quad \begin{matrix} \mathbf{Z} \\ n^2 \times s \end{matrix} = \begin{matrix} \mathbf{T}_{11}^* \\ n^2 \times n^2 \end{matrix} \begin{matrix} \boldsymbol{\Psi} \\ n^2 \times s \end{matrix}$$

Figure 9 reports experiments compressing and factorizing  $\mathbf{T}_{11}$  using the RSRS algorithm which only accesses the matrix through its action on vectors. The PDE is Poisson, and the slab thickness is fixed as  $b = 10$  for various problem sizes  $N = n^2$ .



(A) Time to compute  $\mathbf{T}_{11}^{-1}$  scales linearly.

(B) Memory to store  $\mathbf{T}_{11}^{-1}$  scales linearly.

(C) Number of samples needed is independent of  $N$ . not deteriorate with increasing  $N$ .

(D) The computed factorization is accurate and does

FIGURE 9. The figures above show the effectiveness of using RSRS on a sparse Schur complement  $\mathbf{T}_{11}$  which arises while computing sparse direct solvers for discretized PDEs. The number of samples needed to construct a factorization  $\mathbf{T}_{11}^{-1}$  is constant as  $N$  increases and instead depends only on the desired user tolerance as well as the leaf size  $m$ . For  $\text{atol}=5\text{e-}2$  and  $5\text{e-}4$ , the leaf size  $m$  is set as  $m = 200$ . For  $\text{atol}=5\text{e-}6$ , the leaf size  $m$  is set as  $m = 350$ .

## 7. CONCLUSIONS

The manuscript introduces the algorithm Randomized Strong Recursive Skeletonization (RSRS) for simultaneously compressing and inverting an  $\mathcal{H}^2$ -matrix, given a means of applying the matrix and its adjoint to vectors. RSRS is immediately applicable in a range of important environments, and the numerical results demonstrate the effectiveness of the approach on Schur complements which arise while factorizing a sparse direct solver. It extends the range of the SRS algorithm using tailored approaches for randomized linear algebra applied to rank structured matrices.

**Acknowledgments.** The work reported was supported by the Office of Naval Research (N00014-18-1-2354), by the National Science Foundation (DMS-1952735, DMS-2012606, and DMS-2313434), and by the Department of Energy ASCR (DE-SC0022251).

## REFERENCES

- [1] Patrick Amestoy, Alfredo Buttari, Jean-Yves l'Excellent, and Theo Mary. On the complexity of the block low-rank multifrontal factorization. *SIAM Journal on Scientific Computing*, 39(4):A1710–A1740, 2017.
- [2] Mario Bebendorf. *Hierarchical matrices*, volume 63 of *Lecture Notes in Computational Science and Engineering*. Springer-Verlag, Berlin, 2008. A means to efficiently solve elliptic boundary value problems.
- [3] Steffen Börm. *Efficient numerical methods for non-local operators*, volume 14 of *EMS Tracts in Mathematics*. European Mathematical Society (EMS), Zürich, 2010.  $\mathcal{H}^2$ -matrix compression, algorithms and analysis.
- [4] Chao Chen and Per-Gunnar Martinsson. Solving linear systems on a gpu with hierarchically off-diagonal low-rank approximations. In *Proceedings of the International Conference on High Performance Computing, Networking, Storage and Analysis, SC '22*. IEEE Press, 2022.
- [5] Yijun Dong and Per-Gunnar Martinsson. Simpler is better: a comparative study of randomized pivoting algorithms for cur and interpolative decompositions. *Advances in Computational Mathematics*, 49, 08 2023.
- [6] A Gillman, S Hao, and PG Martinsson. Short note: A simplified technique for the efficient and highly accurate discretization of boundary integral equations in 2d on domains with corners. *Journal of Computational Physics*, 256:214–219, 2014.
- [7] Adrianna Gillman, Patrick Young, and Per-Gunnar Martinsson. A direct solver  $o(n)$  complexity for integral equations on one-dimensional domains. *Frontiers of Mathematics in China*, 7:217–247, 2012. 10.1007/s11464-012-0188-3.
- [8] L. Greengard and V. Rokhlin. A fast algorithm for particle simulations. *J. Comput. Phys.*, 73(2):325–348, 1987.
- [9] Leslie Greengard and Vladimir Rokhlin. A new version of the fast multipole method for the Laplace equation in three dimensions. In *Acta numerica, 1997*, volume 6 of *Acta Numer.*, pages 229–269. Cambridge Univ. Press, Cambridge, 1997.
- [10] Nathan Halko, Per-Gunnar Martinsson, and Joel A. Tropp. Finding structure with randomness: Probabilistic algorithms for constructing approximate matrix decompositions. *SIAM Review*, 53(2):217–288, 2011.
- [11] K.L. Ho and L. Greengard. A fast direct solver for structured linear systems by recursive skeletonization. *SIAM Journal on Scientific Computing*, 34(5):2507–2532, 2012.
- [12] James Levitt. *Building rank-revealing factorizations with randomization*. PhD thesis, University of Texas at Austin, 2022.
- [13] James Levitt and Per-Gunnar Martinsson. Linear-complexity black-box randomized compression of hierarchically block separable matrices, 2022.
- [14] Edo Liberty, Franco Woolfe, Per-Gunnar Martinsson, Vladimir Rokhlin, and Mark Tygert. Randomized algorithms for the low-rank approximation of matrices. *Proc. Natl. Acad. Sci. USA*, 104(51):20167–20172, 2007.
- [15] L. Lin, J. Lu, and L. Ying. Fast construction of hierarchical matrix representation from matrix-vector multiplication. *Journal of Computational Physics*, 230(10):4071 – 4087, 2011.
- [16] Per-Gunnar Martinsson. A fast direct solver for a class of elliptic partial differential equations. *J. Sci. Comput.*, 38(3):316–330, 2009.
- [17] Per-Gunnar Martinsson. Compressing rank-structured matrices via randomized sampling. *SIAM Journal on Scientific Computing*, 38(4):A1959–A1986, 2016.
- [18] Per-Gunnar Martinsson. *Fast Direct Solvers for Elliptic PDEs*, volume CB96 of *CBMS-NSF conference series*. SIAM, 2019.
- [19] Per-Gunnar Martinsson. *Fast direct solvers for elliptic PDEs*. SIAM, 2019.
- [20] Per-Gunnar Martinsson, Vladimir Rokhlin, and Mark Tygert. A randomized algorithm for the decomposition of matrices. *Appl. Comput. Harmon. Anal.*, 30(1):47–68, 2011.
- [21] Per-Gunnar Martinsson and Joel A. Tropp. Randomized numerical linear algebra: Foundations and algorithms. *Acta Numerica*, 29:403–572, 2020.

- [22] P.G. Martinsson. A fast randomized algorithm for computing a hierarchically semiseparable representation of a matrix. *SIAM Journal on Matrix Analysis and Applications*, 32(4):1251–1274, 2011.
- [23] P.G. Martinsson and V. Rokhlin. A fast direct solver for boundary integral equations in two dimensions. *J. Comp. Phys.*, 205(1):1–23, 2005.
- [24] E. Michielssen, A. Boag, and W. C. Chew. Scattering from elongated objects: direct solution in  $O(N \log^2 N)$  operations. *IEE Proc. Microw. Antennas Propag.*, 143(4):277 – 283, 1996.
- [25] Victor Minden, Kenneth L. Ho, Anil Damle, and Lexing Ying. A recursive skeletonization factorization based on strong admissibility. *Multiscale Modeling & Simulation*, 15(2):768–796, 2017.
- [26] Yuji Nakatsukasa. Fast and stable randomized low-rank matrix approximation, 2020. arxiv.org report #2009.11392.
- [27] Daria Sushnikova, Leslie Greengard, Michael O’Neil, and Manas Rachh. Fmm-lu: A fast direct solver for multi-scale boundary integral equations in three dimensions, 2022.
- [28] Toru Takahashi, Pieter Coulier, and Eric Darve. Application of the inverse fast multipole method as a preconditioner in a 3d helmholtz boundary element method. *Journal of Computational Physics*, 341:406–428, 2017.
- [29] J. Xia, S. Chandrasekaran, M. Gu, and X.S. Li. Fast algorithms for hierarchically semiseparable matrices. *Numerical Linear Algebra with Applications*, 17(6):953–976, 2010.
- [30] Jianlin Xia, Shivkumar Chandrasekaran, Ming Gu, and Xiaoye S. Li. Superfast multifrontal method for large structured linear systems of equations. *SIAM J. Matrix Anal. Appl.*, 31(3):1382–1411, 2010.
- [31] Anna Yesypenko and Per-Gunnar Martinsson. Slablu: A two-level sparse direct solver for elliptic pdes. *arXiv preprint arXiv:2211.07572*, 2022.